Proceeding of SPIE, 2004, paper 5323-55

Multichannel multiphoton imaging of metal oxides particles in biological system

Yuangang Zheng, Gary Holtom* and Steven Colson

Environmental molecular science laboratory, Pacific Northwest National Laboratory, Richland, WA 99352

*Correspondence: Email: gary_holtom@pnl.gov;
WWW: http://pnlxnotes3.pnl.gov/bios/Biosketch.nsf/ByNameInit/holtom_gr;
Telephone: 509 376 5331; Fax: 509 376 6066

Abstract

Near-IR ultrafast pulse laser and confocal microscope are combined to create a multiphoton multichannel non-linear imaging technique, which allows *in situ* 3-D characterization of nonfluorescent nanoparticles in biological systems. We observed intense CARS signals generated from various metal oxides due to their high third-order nonlinear susceptibilities ($\chi^{(3)}$), which do not depend on the vibrational resonance but on the electronic resonance. We show that fine and ultrafine particles of metal oxides in alveolar macrophage cells may be imaged *in vitro* using CARS and multiphoton fluorescence microscopy with highest optical resolution for extended periods without photobleaching effects. The advantage of the epi-detection over the forward detection for imaging sub-micron particles has been investigated.

Introduction

CARS microscopy and other multiphoton imaging methods are emerging as new tools for imaging organic species in biological systems utilizing the non-linear optical properties of molecules[1-3]. Using strongly focused laser beams, multiphoton imaging method is well suited for three-dimensional imaging since all of the intensity results from a single sample plane with a thickness on the order of one micrometer. Generated by a four-wax mixing process, the intensity of CARS signal is dependent on the third-order nonlinear susceptibility $\chi^{(3)}$ of the molecule, which consists of two major contributions from electronic resonance and vibrational resonance. The background signal from electronic resonance and media could be effectively minimized to enhance the vibrational contrast by using near-IR excitation laser pulse and different detection techniques such as epi-detection[4], polarization detection[5] and time-resolved detection[6]. Unlike the imaging of organic species, the overall CARS intensity from a variety of metal oxides is surprisingly larger by a few orders of magnitude compared with that of organic species. In addition, the CARS intensity due to the electronic contribution is substantially independent of the Stokes shift, or vibrational resonance. This allows us to minimize the vibrational contribution from the media to a negligible level by tuning the pump and Stokes beams, and maximize the electronic contribution to image the nonfluorescent metal oxides particles, even for particles smaller than the diffraction limit of an optical microscope with good signal to noise ratio. We have applied CARS microscopy in imaging these metal oxides nanoparticles (ZnO, TiO_2 and Fe_2O_3) in alveolar macrophage cells *in vitro*.

Zinc oxide nanoparticle has been used as in transparent sun-screens and cosmetics due to its superior absorbance of UV light for skin protection. TiO_2 nanoparticle, another commercialized nanoparticle, is used not only in sunscreens, but also in self-cleaning glass, flat-screen displays, antibacterial coatings and photo catalysts[7]. The researches showed that these nanoparticles could get into the human body by inhalation or dermal absorption and might exert the cytotoxicity[8]. Iron oxide nanoparticles are introduced into human tissues by magnetic resonance imaging (MRI) technique for medical diagnostics, and also widely used as host agent for target-oriented drug delivery. Unlike coarse particles, nanoparticles cannot be imaged by conventional optical techniques. The 3-D CARS microscopy provides a unique opportunity to image the entry route and whereabouts of these nanoparticles in tissue, which is very important for investigating their physiological function *in vivo*.

There are two common features for ZnO, TiO_2 and Fe_2O_3, making them suitable for CARS microscopy. Firstly, all these three metal oxides are among the most promising materials for large third-order nonlinear characteristics. CARS microscopy has proven a powerful imaging tool in high optical selectivity and sensitivity especially for the samples with large third-order nonlinearity. The reported values of $\chi^{(3)}$ are 4×10^{-12} esu for TiO_2[9]; $2.1 \times 10^{-11} \sim 4 \times 10^{-10}$ esu for iron oxides[10]; and 2×10^{-12} esu for zinc oxide[11], much higher than 2.8×10^{-14} esu for silica glass[9]. The high sensitivity and great contrast for these metal oxides nanoparticle against the cover slip in our CARS microscopy can be well explained by the fact that their $\chi^{(3)}$ is hundreds of times higher than that of SiO_2. It is notable that $\chi^{(3)}$ of the doped or capped metal oxides nanoparticles could increase by many orders of magnitude, up to 2×10^{-6} esu for the Au/ZnO composite film[11], consequently generating much more intense CARS signal than pure materials, making these nanoparticles candidates for non-bleaching optical labels for biological imaging like quantum dots.

Secondly, all these three metal oxides are defined as wide bandgap semiconductors. The wavelengths of bandgap absorption for ZnO, TiO_2 and Fe_2O_3 are 370, 400 and 550 nm, respectively. Our experiments showed that the CARS signals of these particles are relatively independent of the frequency shift of Stokes beam but their normalized intensities vary by more than one order of magnitude as the pump beam is tuned from 780 to 870 nm. This observation confirmed that the CARS intensity was dominated by the two-photon electronic resonance related to the bandgap transition. We found the CARS signal of each oxide could be maximized by tuning the frequency of pump beam.

In addition, unlike nonfluorescent TiO_2 and Fe_2O_3, ZnO exhibits a characteristic fluorescence spectrum with a maximum around 500 nm. Multiphoton fluorescence of ZnO particles are detected in the wide range of 450~550 nm with Ti:Sapphire laser excitation following a nonlinear power rule. In this work, the CARS and multiphoton fluorescence images were taken simultaneously to identify the ZnO particles embedded in the iron oxide film.

Materials and Methods

Chemical materials

TiO_2 fine particle was purchased from Fluka (PN. 72562, anatase form, the average geometry size is 500 nm). TiO_2 nanoparticle (PM25, a mixture of anatase and rutile form, ~40 nm) was purchased from Degussa AG, Germany. ZnO fine particle (~1 μm) was purchased from Sigma. Fe_2O_3 nanoparticle (30~50 nm) was purchased from Nanostructured & Amorphous Materials, INC. All the particles was prepared in 1 mg/ml water suspension and sonicated for 30 minutes before the cell treatment.

Cell treatment

The macrophage cells were grown in 10% FBS media (450 ml RPMI medium 1640, 50 ml fetal bovine serum and 5 ml 100x penicillin/streptomycin) and treated with 2μg/ml ultrafine or fine particles followed by 24 hours incubation. The treated cells were fixed with 75% methanol and 25% acetic acid at 4 degree for 5 minutes. All the cells were grown and treated in culture dish with glass bottom in 0.17 mm thickness.

CARS microscopy

Our CARS microscope used a pair of picosecond-width lasers operating at a repetition rate of 250 KHz. It has been modified by addition of a high repetition rate OPA (Coherent Rega) to allow convenient access to a very wide vibrational range[12] (from 500 to 3300 cm^{-1}) and for photon counting[13]. To minimize the vibrationally resonant CARS signal from the cover clip and the cell, we tune the energy difference between the pump beam and Stokes beam to 2300 cm^{-1}, since there is no vibrational band around this frequency for most organic species and silica glass. For all the images, the pump laser is set to 810 nm and the Stokes beam from OPO is tuned to 980 nm, the anti-Stokes signal is detected at 690 nm with two narrow band filters.

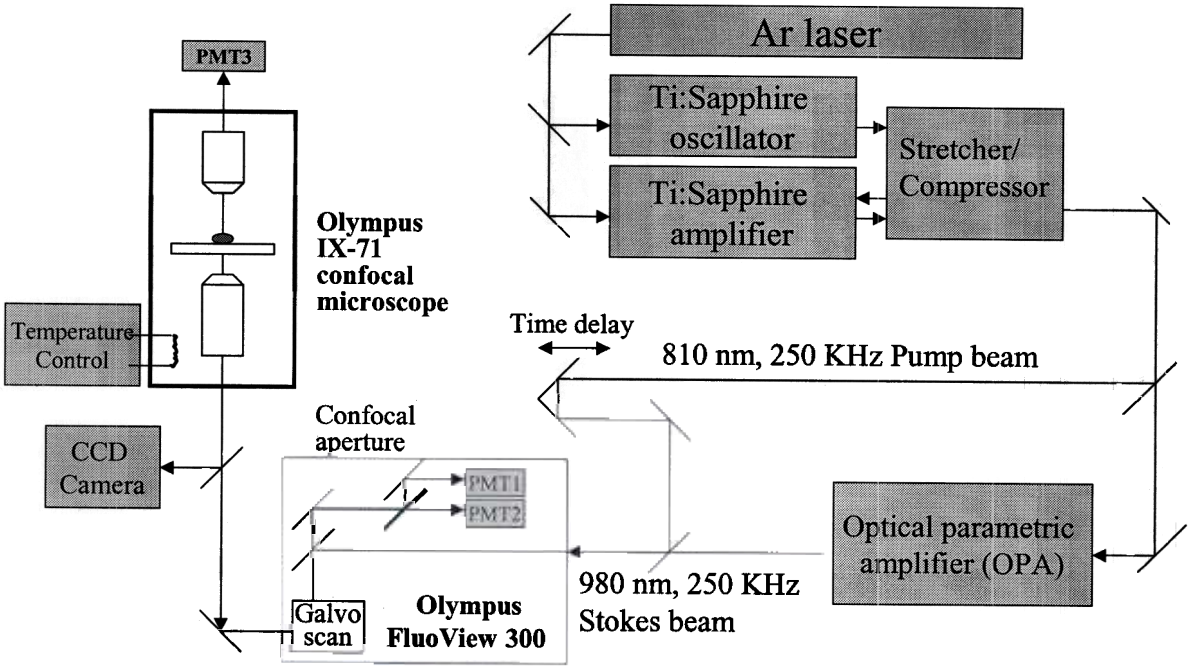

Figure 1: Instrumental setup

A major modification of our system is to use an Olympus IX-71/FV300 confocal microscope as shown in Figure 1. The Olympus IX-71 confocal microscope has multiple detection geometries to permit the traditional transmitted (forward) CARS detection, as well as the recently described variants for epi-detection[4] (backward). The epi-detected CARS have advantages over the transmitted CARS for reducing the background signals from the bulk media that reduce the contrast of small particles embedded in thicker structures. The ratio of forward and backward CARS signal is close to one for a spherical sample with diameter of $0.1\lambda_{pump}$, but for the bulk solvent this ratio is up to 10,000[4], so that epi-detection is the preferred geometry for the CARS imaging of nanoparticles.

With multi-channel operating capability of FV300 software package, we use one forward-detection channel and two epi-detection channels. The photons were detected by either the fluorescence channel or CARS channel after being separated with a 570 nm dichroic mirror.

All images were acquired with a 60x water-immersion Olympus objective (NA 1.2). The normal scan time is 9 seconds for a 1024 x 1024 pixels XY image; the dwelling time on each pixel is 8 μs. The average pump and Stokes powers near the focusing plane were measured as 5 mW and 3 mW, respectively. Our experiments show that the macrophage cells stay in the good condition and appear healthy after a complete 3-D scan.

Results and Discussions

Epi-detection *vs* forward detection:

To evaluate the advantage of backward (Epi) detection over the forward (For) detection for CARS imaging of nanoparticles, we took both the Epi-CARS and For-CARS images of same single macrophage cell treated with Fe_2O_3 nanoparticles as shown in Figure 2. All the laser power and detector sensitivity are kept the same to ensure an accurate comparison of signal-to-noise ratios. Both the E-CARS and F-CARS methods generate a clear image of Fe_2O_3 nanoparticles with similar resolution and sensitivity. The average CARS intensity of Fe_2O_3 particles in the forward detection is slightly higher than the intensity obtained by the epi-detection. The contrast in Epi-CARS image is apparently higher than For-CARS image, in which an outline of macrophage cell is faintly visible in all four stacks. The gain in contrast should be attributed to the minimization of the background signal from the cell, which is composed of organic species.

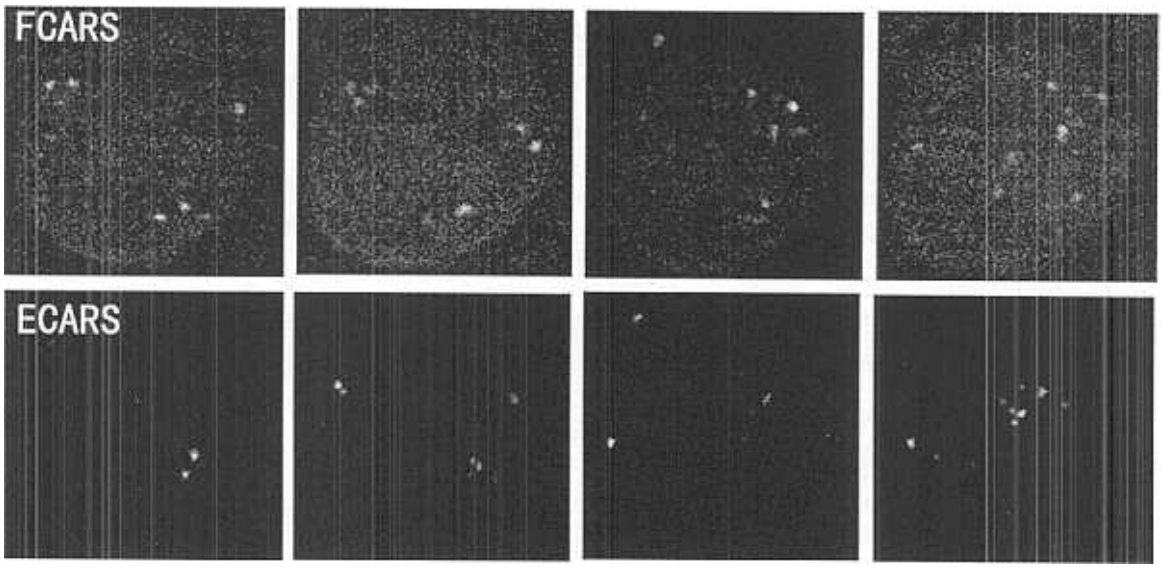

Figure 2: Comparison of For-CARS and Epi-CARS images of Fe_2O_3 nanoparticles treated live macrophage cell. The dimension of the full image is 10 x 10 μm. The images were taken on four consecutive stacks in 1 μm stepwise.

To evaluate the preferred imaging method, it is important to directly compare the CARS signal from metal oxides particles obtained from epi-detection and forward-detection. Our study showed that the forward CARS signals from the nanoparticles are generally higher by a factor of 1~2 than epi-CARS signals. We prepared a composite sample by mixing 1 mg/ml 1-μm ZnO particles with hydrous ferric oxides (HFO) solution and made a thin film by dehydration. The CARS images of one piece of HFO film with ZnO particles embedded were taken in forward and backward detection methods, as shown in Figure 3A and 3C, respectively. The multiphoton fluorescence signals were detected simultaneously to prove the presence of embedded ZnO particles as shown in Figure 3B and 3D. The CARS signals of HFO dominate the forward CARS

image (Fig. 3A). The F-CARS image shows some vacancies inside the HFO film, which can be assigned as ZnO particles by their co-localization with bright spots in the multiphoton fluorescence images (Fig. 3B and 3D). The most prominent observation is: All those black holes inside the HFO film seen in For-CARS are inverted to brighter spots the HFO film in the Epi-CARS image (Fig. 3C). To better understand the difference between Epi-CARS and For-CARS images, we should point out that the background signal from the media (glass and water) is reduced by at least a factor of 15, from 150 counts/pixel in For-CARS image to <10 counts/pixel in Epi-CARS image. Signals from the ZnO particles are in the range of 150-200 counts/pixel in both the For-CARS and Epi-CARS images. But for the bulk HFO film, the average CARS signal correspondingly changes from 250 counts/pixel to 100 counts/pixel. Thus, the inversion of contrast is actually a consequence of the particle-to-bulk effects.

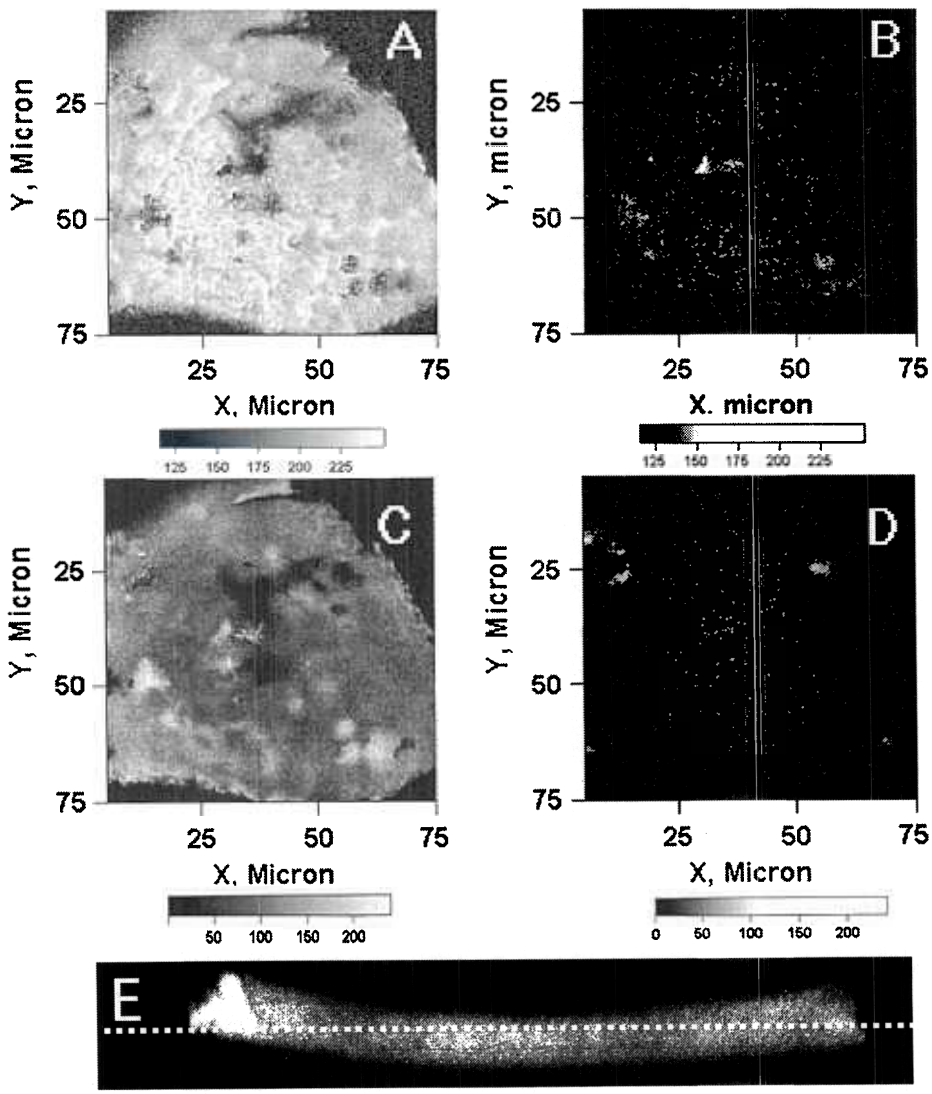

Figure 3: Comparison of epi-detection and forward detection of ZnO particles embedded HFO film. A, Forward CARS image, B, Forward multiphoton fluorescence image; C, Epi-CARS image; D. Epi multiphoton fluorescence image; E. XZ Epi-CARS image of HFO film, the dashed white line represents the focus plane for Figure 3A-3D.

It is very interesting that only those ZnO particles near the center are seen in forward fluorescence image (Fig. 3B) while only the ZnO particles near the edge of the film are seen in epi-fluorescence image (Fig 3D). This phenomenon can be rationalized by considering the thickness and shape of HFO film. The typical shape of HFO film is boat-like with a dimension about 100 microns and a thickness of a few microns, which has been confirmed by the 3-D CARS image of HFO film (a slice of XZ image in Fig. 3E shows the thickness and the shape of HFO film). The bulk, opaque HFO film could absorb the fluorescence from ZnO particles. At the focus plane for Figure 3A-3D, ZnO particles near the center are largely exposed to the top surface of the film, while the particles near the edge are exposed to the bottom surface of the HFO film. The particle position, relative to the HFO film, may allow or prohibit the fluorescence photons generated in the HFO film to reach the detector. When ZnO particle is completely buried the fluorescence signal will be totally blocked. However, the far-red CARS signal at 690 nm of ZnO particle is not significantly blocked by HFO film no matter where it is buried or exposed. These experimental observations and interpretations should be taken into consideration for 3-D characterization of opaque materials and thick tissues.

Comparison of SEM and CARS image

We treated the macrophage cells with TiO_2 and Fe_2O_3 nanoparticles for 8 hours and fixed the treated cell with methanol/acetic acid. The Epi-CARS and SEM images were taken for the same group of cells, as shown in Figure 3. The SEM image of TiO_2 treated cells (Fig. 4A) doesn't generate any meaningful contrast for nanoparticles. Some Fe_2O_3 lumps are discernible in SEM image (Fig. 4C) but the contrast is very poor. In CARS image (Fig. 4B and 4D) we are able to identify individual TiO_2 or Fe_2O_3 nanoparticle embedded in the cellular matrix with very high contrast. It is quite impressive that two big lumps shown in SEM image of Fe_2O_3 treated cells (Fig. 4C) are not seen in the CARS image (Fig. 4D), because they are not Fe_2O_3 particles, most likely buffer salt crystals. The intensity profile (not shown) demonstrates that the signal-to-noise ratio is up to 15 for TiO_2 and Fe_2O_3 nanoparticles. Although the resolution is insufficient to characterize each single nanoparticle, the CARS resolution is still comparable with the best conventional optical microscopies at the 800 nm region.

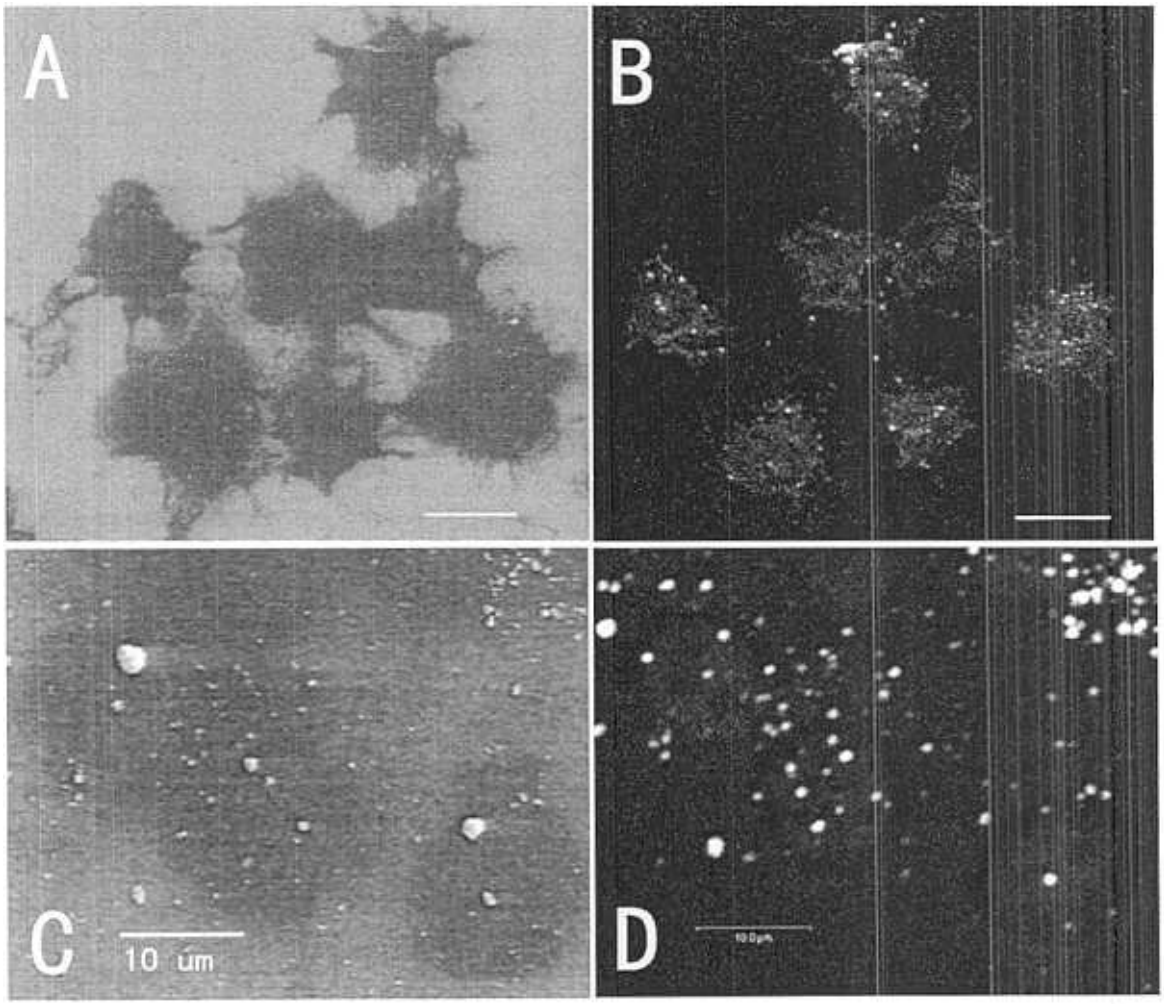

Figure 4: Comparison of SEM and CARS images of fixed macrophage cells treated with TiO_2 and Fe_2O_3 nanoparticles. A. SEM image of TiO_2 treated cells, magnification: 500x; B. CARS image of TiO_2 treated cells; C. SEM image of Fe_2O_3 treated cells, magnification: 500x; D. CARS image of Fe_2O_3 treated cells. All the scale bars represent 10 μm.

3-D CARS imaging

With the 3D imaging capability of our CARS microscopy we are able to image TiO_2 fine particles (~500 nm) in treated macrophage cells *in vitro* as shown in Figure 5. The scanning time for each slice is 0.9 second, and the complete scan of 40 slices took less than 1 minute. The intensity profile shows that the spatial resolution is about 500 nm, which we take to be the diffraction limit. The axial resolution was measured as 900 nm. The average signal-to-noise ratio is larger than 10 against the cell. This 3-D visualization provides us with new insights to study the cellular response of the macrophages or other tissues to potentially toxic nonfluorescent nanoparticles without the needs of labeling.

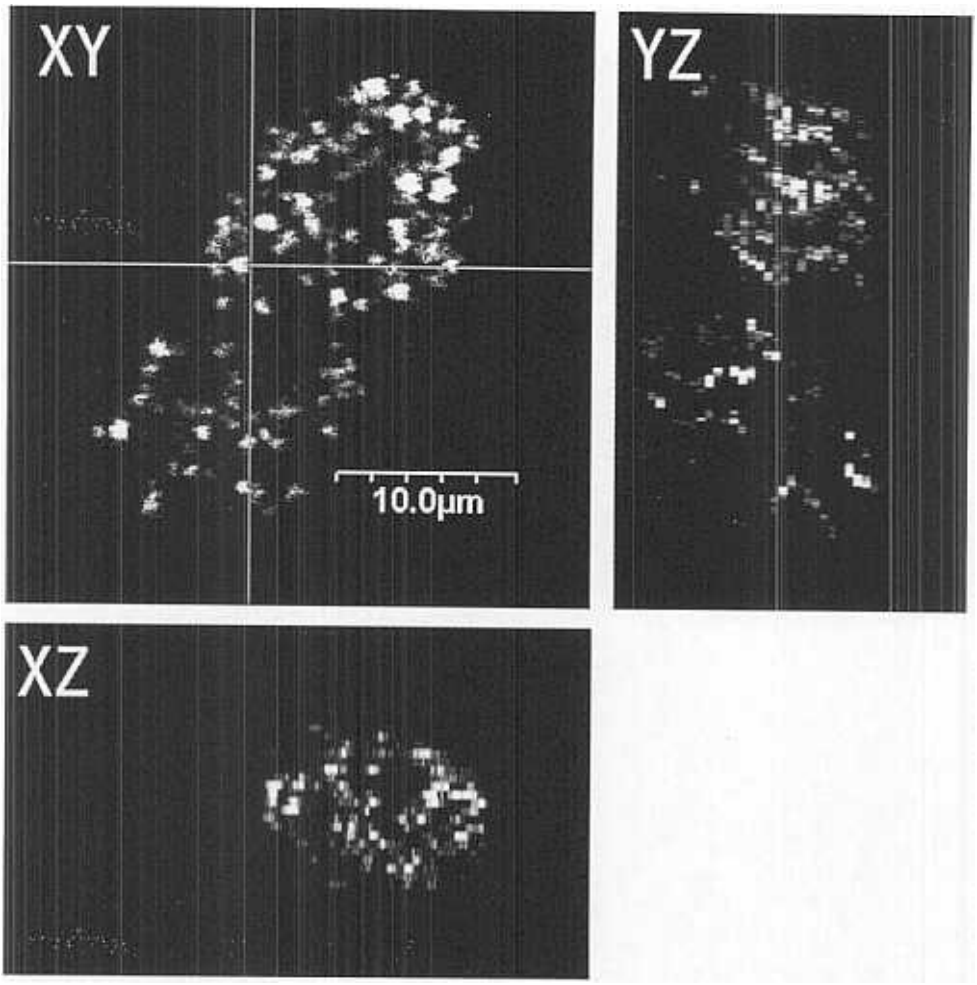

Figure 5: 3-D CARS image of TiO_2 fine particles treated macrophage cells. The scanning volume is 30 x 30 x 20 μm, stepsize: 0.5 μm.

With the great optical contrast and sensitivity, the CARS microscopy technique is a unique 3-D imaging tool for the nonfluorescent inorganic nanoparticles in a biological matrix. Currently we are applying the CARS microscopy on a variety of biological systems to realize its potentials in biological imaging.

Acknowledge:

The research described in this manuscript was performed at the W.R. Wiley Environmental Molecular Sciences Laboratory, a national scienctific user facility sponsored by the U.S Department of Energy's office of Biological and Environmental Research and located at Pacific Northwest National Laboratory. PNNL is operated for the Department of Energy by Battelle.

Reference

1. Zumbusch, A., Holtom, G., & Xie, X. (1999) *Phys. Rev. Lett.* **82**, 4142-4145.
2. Cheng, J., Pautot, S., Weitz, D., & Xie, X. (2003) *Proc. Natl. Acad. Sci. USA* **100**, 9826-9830.

3. Larson, D., Zipfel, W., Williams, R., Clark, S., Bruchez ,M., Wise, F., & Webb, W. (2003) *Science* **300**, 1434-1436.
4. Volkmer, A., Cheng, J., & Xie, X. (2001) *Phys. Rev. Lett.* **87**, 23901-23904.
5. Cheng, J., Book, L., & Xie, X. (2001) *Optics Lett.* **26**, 1341-1343.
6. Volkmer, A., Book, L., & Xie, X. (2002) *Appl. Phys. Lett.* **80**, 1505-1507.
7. *Size Matters--No small matter II: the case for a global moratorium*, (2003) Occasional paper series, ETC group.
8. Colvin V. (2003) *Nature Biotechnology* **21**, 1168-1172.
9. Liao, H., Xiao, R., Wang, H., Wong, K., & Wong, G. (1998) *Appl. Phys. Lett.* **72**, 1817-1819.
10. Hashimoto, T., Yamada, T., & Yoko, T., (1996) *Journal of Applied Physics* **80**, 3184-3190.
11. Liao, H., Wen, W., Wong, G., & Yang, G. (2003) *Optics Letters* **28**, 1790-1792.
12. Holtom, G., Thrall, B., Weber, T., Zhu, L., Hopkins, D., Parkinson, C., Colson, S., Price, J., Chin, B., Choi, A., & Risby, T. (2001) *Proc. SPIE* **4262**, 319-328.
13. Holtom, G., Thrall, B., Chin, B., et al (2001) *Traffic* **2**, 781-788.